Nedeljko Vukojević[1], Zlatan Ištvanić[2], Fuad Hadžikadunić[1], Amna Bajtarević-Jelač[1]*

INFLUENCE OF INCREMENTAL SHEET FORMING AND PWHT ON THE STRUCTURAL INTEGRITY OF VESSEL HEADS MADE OF STEEL P355NL2+H

UTICAJ INKREMENTALNOG OBLIKOVANJA LIMA I TERMIČKE OBRADE POSLE ZAVARIVANJA NA INTEGRITET KONSTRUKCIJE DANCA POSUDE OD ČELIKA P355NL2+H

Originalni naučni rad / Original scientific paper
UDK /UDC:

Rad primljen / Paper received: 1.10.2023

Adresa autora / Author's address:
[1)] University of Zenica, Faculty of Mechanical Engineering, Fakultetska 1, 72000 Zenica, Bosnia and Herzegovina (B&H)
[*]email: nedeljko.vukojevic@unze.ba
[2)] Metacomm Jajce d.o.o., Bage 5, 70101 Jajce, B&H

Keywords
- welded vessel heads
- incremental sheet forming (ISF)
- steel P355NL2+H
- structural integrity
- post weld heat treatment (PWHT)
- residual stress

Ključne reči
- zavarena danca
- inkrementalno oblikovanje limova
- čelik P355NL2+H
- integritet konstrukcija
- termička obrada posle zavarivanja
- zaostali naponi

Abstract

Incremental sheet forming (ISF) of torispherical vessel heads causes hardening of surface layers. The strengthening of the material can cause formation of initial cracks, and in combination with welding and residual stresses can cause the appearance of brittle fracture. The focus of the research is the heat-affected zone (HAZ) in the welded joint. Post weld heat treatment can reduce but also increase negative effects, as is the subject of analysis in this paper. Experimental research was carried out on a sheet of high-quality steel grade P355NL2+H. Research included determining actual mechanical properties of the welded joint, impact energy testing, hardness testing, measurement of residual stresses, as well as fracture mechanics tests on samples taken from the welded joint zone of finally formed vessel heads. An integrity assessment procedure was carried out for the assumed values of internal pressure and for a hypothetical crack on the outer contour of the vessel head, and the results are presented graphically (failure assessment diagram). Analyses were carried out on samples taken from finished vessel heads, before and after normalisation.

Izvod

Inkrementalno oblikovanje lima (ISF) torisferičnih danaca uzrokuje otvrdnjavanje površinskih slojeva. Ojačanje materijala može uzrokovati nastanak početnih prslina, a u kombinaciji sa zavarivanjem i zaostalim naponima može izazvati pojavu krtog loma. Fokus istraživanja je zona uticaja toplote (ZUT) u zavarenom spoju. Primenom termičke obrade posle zavarivanja može se uticati na smanjenje, ali i na povećanje negativnih učinaka, što je predmet analize u ovom radu. Eksperimentalna istraživanja sprovedena su na limu od visokokvalitetnog čelika klase P355NL2+H. Istraživanje je obuhvatilo utvrđivanje stvarnih mehaničkih svojstava zavarenog spoja, merenje tvrdoće, merenje zaostalih napona, kao i ispitivanja mehanike loma na uzorcima uzetim iz zone zavarenog spoja konačno oblikovanih danaca. Sproveden je postupak procene integriteta za usvojene vrednosti unutrašnjeg pritiska i hipotetičke prsline na spoljašnjoj konturi danca, a rezultati su prikazani u grafičkom obliku (dijagram procene loma). Analize su sprovedene na uzorcima uzetim iz gotovih danaca pre i posle termičke obrade normalizacijom.

INTRODUCTION

Incremental sheet forming (ISF) is a process of metal forming by progressive local plastic deformation. Shaping is done by moving the tool along the contour of the work piece, gradually shaping it as desired. The technique of processing by incremental deformation was developed in Japan, and the first published works in the field of gradual forming, primarily by Japanese researchers, dates from the early 90s of the 20th century, /1, 2/.

The mechanical action of the tool leads to large plastic deformations and causes deformation strengthening which certainly causes the appearance of initial cracks, /3/. The strengthening of surface layers in combination with increased thickness of the part and residual stresses /4, 5/ creates conditions for brittle fracture.

The action of the tool is not continuous over the entire surface of the future vessel head. The directional action of the tool leads to different properties in the material at the local level, resulting in a non-uniform distribution of properties. This phenomenon is not suitable from the aspect of safety under the action of operating load. Different thicknesses of basic sheets as well as the number of pressing operations can cause different effects in the material, /6/. The number of pressing operations and the size of the tool radius have the highest influence on the magnitude and distribution of residual stresses, /7/.

METHODS

Pressure vessel heads are made from one piece, but the standards also allow them to be made in a welded version when vessel head dimensions are larger than standard sizes of sheets for production, /8-10/. The selected material is a high-quality steel for pressure vessels grade P355NL2+H. Sheets of 10 mm thickness are welded with a double-sided

full penetration butt weld. The tests are focused on the heat-affected zone (HAZ). The vessel head is treated by post-weld heat treatment (PWHT) - normalisation, with the aim of reducing residual stresses. Experimental research includes:
– measuring residual stresses,
– hardness tests,
– tensile tests,
– impact energy tests,
– fracture mechanics tests, and
– structural integrity assessment.

Material, welding, and manufacturing technology

Chemical composition of the base material P355NL2+H for the manufacture of vessel heads is presented in Table 1.

Table 1. Chemical composition of the base material.

	Chemical elements (wt. %)									
t (mm)	C	Si	Mn	P	S	Al	Cr	Ni	Mo	Cu
10	0.17	0.32	1.16	0.006	0.007	0.03	0.022	0.26	0.017	0.157

The carbon equivalent for the selected samples is calculated using the Ito-Bessyo equation, /4/:

$$C_E = C + \frac{Mn}{20} + \frac{Mo}{15} + \frac{Ni}{60} + \frac{Cr}{20} + \frac{V}{10} + \frac{Cu}{20} + \frac{Si}{30} + 5B\,. \qquad (1)$$

The carbon equivalent for the selected samples is presented in Table 2.

Table 2. C-equivalent of P355NL2+H.

sheet	according to material certificate	according to Eq.(1)
10 mm	C_E = 0.4	C_E = 0.26

Considering that the base material has good weldability, the EN ISO4063-121 (EPP/UP) welding procedure shown in Table 3 was used for joining the sheet metal, /11/.

Table 3. Welding procedure.

Additional and auxiliary material		Preheating temperature	≥100 °C
Name and manufact.	ESAB Ok Auto rod 13.40	Interlayer temperature	200 °C
Classific.	EN14171-A-S3Ni1Mo	PWHT	930 ± 40 °C
Type of lining	÷	Work technique	Manual
Wire diameter	∅3.0 mm	Max. passage width/ layer no.	15-17 mm/2
Drying	2h/350 °C	Initial and intermediate cleaning	Grinding and brushing
Powder	OK-Flux 10.62	Other things	÷
Remark	Standard: EN14171-A /21/		

Experimental samples are made by incremental sheet forming from initially welded round sheets. The observed phenomenon of sheet thinning is especially pronounced in thicker sheets. This phenomenon also causes an increase in thickness towards the outer edges of the heads due to the extrusion of material during the construction of the torus part. The vessel head is made in accordance with DIN 28013 (ellipsoidal dished ends), /12/. The incremental deformation of the basic round sheet is performed on a hydraulic press with an exchangeable tool and pressure force. Press type is P2MF 200x4 – 'Sertom', Milano, Italy. Test results are presented in Table 4, /6/.

Normalisation annealing is performed by heating up to 930 ± 40 °C within a 5-hour period, holding for about 0.5 hours and cooling in air.

Table 4. Test results before/after PWHT.

Material properties		Before/After PHWT
Yield stress (MPa)	R_{eH}	538 / 433
Ultimate strength (MPa)	R_m	620 / 591
Elongation (%)	Δ	26 / 20.5
Contraction (%)	*A*	12.7 / 16
Impact energy (J)	KV	136 / 132
Hardness (HV)	weld metal	222 / 236
	HAZ	232 / 202
	base metal	206 / 180
Residual stress φ - direction (MPa)	$\sigma_{res\text{-}\varphi}$	333 / 161

Sampling scheme

A part of the vessel head with a welded joint in the middle was tested, Fig. 1. The sheets are double sided butt-welded. Samples were taken from the outer cylindrical part of the vessel head and from the zones where plastic deformations are the most intense. The samples were taken out as curved panels from the vessel head.

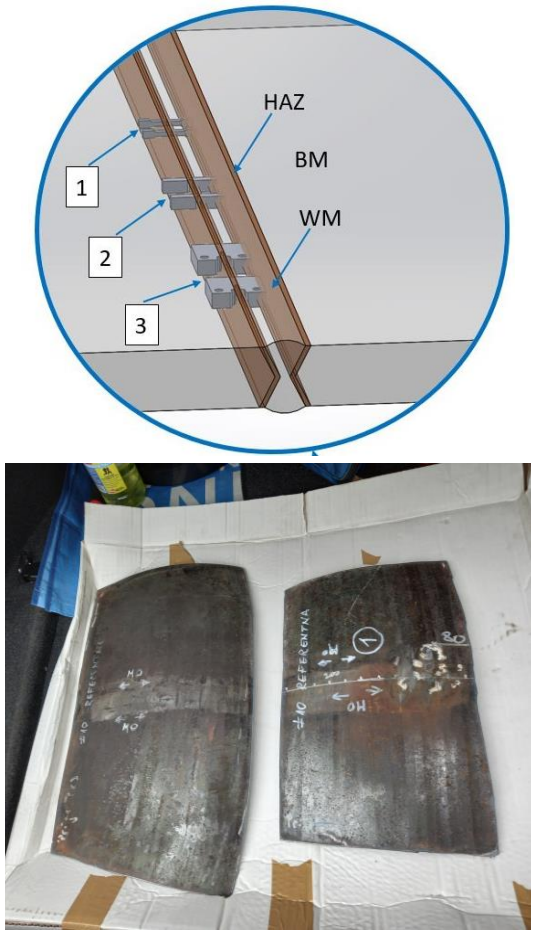

Figure 1. Sampling scheme from the vessel head: tensile specimen -1; Charpy specimen -2; CT specimen -3.

Properties in the heat-affected zone after plastic deformation were determined from test samples taken from the direction transverse to the longitudinal axis of the weld.

Hardness testing

Hardness tests determined significant differences and their possible influence on other mechanical test results. Measurements were made on a device for testing hardness and micro hardness - ZWICK. Hardness tests were performed on the double butt-welded joint cross-section using the Vickers test method, with load of 10 kg (HV1), test temperature 22 °C according to standard BAS EN ISO 6507-1:2018, /13/. Test results of all samples are presented in Table 4.

The hardness test was performed on sample cross section. Hardness test results and a typical schematic representation of impression locations is shown in Figs. 2 and 3.

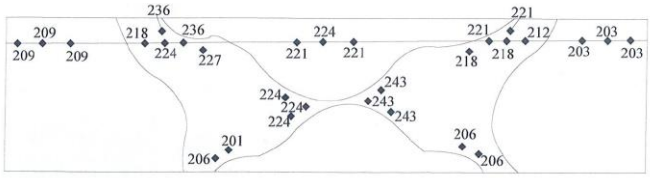

Figure 2. Scheme of hardness locations on a double butt-welded joint before PWHT (magn. 2×).

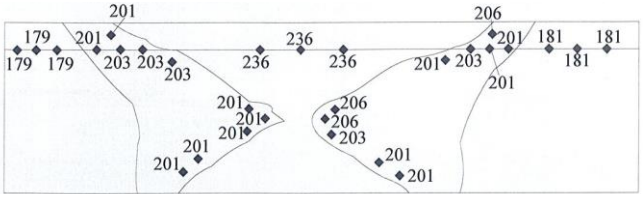

Figure 3. Scheme of hardness locations on a double butt-welded joint after PWHT (magn. 2×).

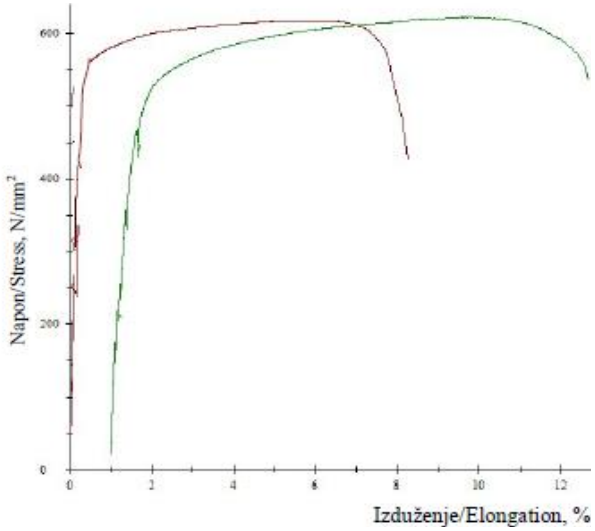

Figure 4. Diagram force-elongation.

Tensile testing

Tensile tests of specimens taken out from the vessel heads were carried out at room temperature +16 °C. The test procedure itself is defined by standard BAS EN ISO 6892-1:2017 B /14/, on tensile test specimens whose geometry is defined by standard BAS EN ISO 4136:2014 /15/. Test specimens are modified with a transverse groove cut in the HAZ zone which is the subject of research. A typical tensile test diagram for a 10 mm sheet is shown in Fig. 4. Results of the tensile tests of the test tubes are presented in Table 4.

Impact energy testing

Impact tests of samples were done at room temperature +20 °C. The test procedure was performed according to BAS EN ISO 148:2016 /16/ on standard test specimens BAS EN ISO 9016:2012 /17/, and using the Charpy pendulum 300 J test machine. Impact energy test results are given in Table 4.

The total absorbed impact energy is obtained before and after PWHT. The plastic deformation strengthening effect is the cause of decreased toughness. In general, the obtained values of total impact energy in HAZ show a significant tendency toward brittle fracture.

Measurement of residual stresses

The measurement of residual stresses is performed using the hole drilling method according to ASTM E837, /18/. Measurements are made in the heat-affected zone, which includes a narrow area next to the very edge of the weld. The location of the strain gauge type 1-RY61-1.5/120 was at places of the highest plastic deformation, Fig. 5. Measurement results are also shown in Table 4.

Figure 5. Position of strain gauge on vessel head.

Before the final conclusions, it should be noted that measurements are made in the HAZ or zones close to HAZ with a relatively small number of measurements for this type of analysis. Values of main residual stresses using Mohr's circle equation are recalculated so that they follow the directions of main operating stresses in the meridional and circular directions. The residual stress in the circular direction σ_φ is used for further analysis in structural integrity assessment.

Determination of fracture mechanics parameter K_{Ic}

Experimentally determined fracture mechanics parameter J-integral can be qualitatively analysed even after significant plastic deformation according to the procedure described in ASTM E1820, /19/, and ASTM E399, /20/. Since the requirements for the plane stain condition are not realised, given by Eq.(2), instead elastic-plastic fracture mechanics is used,

$$B \geq 2.5\left(\frac{K_{Ic}}{R_T}\right)^2 . \qquad (2)$$

For the experimentally determined value of critical J_{Ic}-integral, the value of critical stress intensity factor in plane strain state, K_{Ic}, is calculated using:

$$K_{Ic} = \sqrt{\frac{J_{Ic}E}{1-\nu^2}} . \qquad (3)$$

Tests are performed on a curved sample cut from the bottom of the vessel. Compact tension (CT) specimen was made from the plate, as shown in Fig. 6, with nominal sizes of width and height, but reduced thickness, to obtain a specimen with parallel sides. Actual specimen thickness is 7 mm.

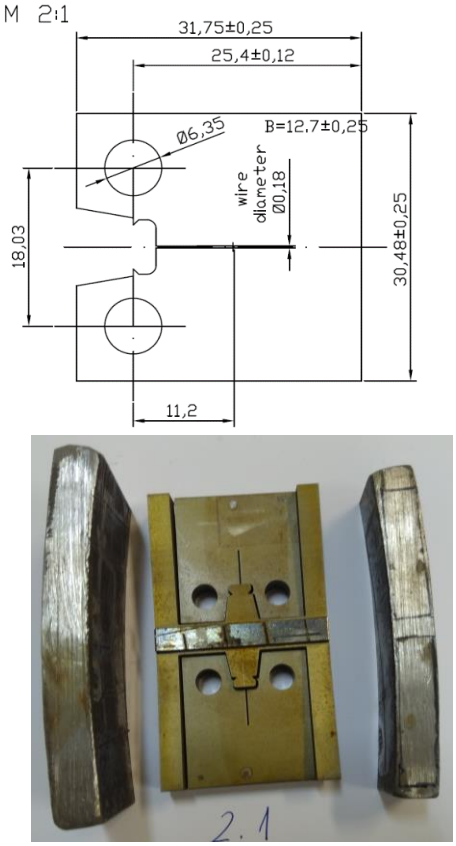

Figure 6. Test specimen for fracture toughness testing

Test specimens are made with a mechanical notch in the HAZ as a critical area of the structure. For further analysis, the lowest measured values of yield stress R_{eH} and tensile strength R_m were taken, Table 4. The test was performed on a computer-controlled servo-hydraulic machine INSTRON 1255 with a dynamic-static loading capacity up to 250 kN, in accordance with ASTM E1820 standard. The INSTRON-CMOD clip gauge is used to measure crack opening. The fracture toughness test is performed at room temperature under displacement control at a speed of v = 1 mm/min.

Figures 7 and 8 show typical diagrams for the tested CT specimen. The procedure for testing fracture behaviour of the CT specimen with a CMOD clip gauge records displacement V (mm) in the force (load-line displacement) direction.

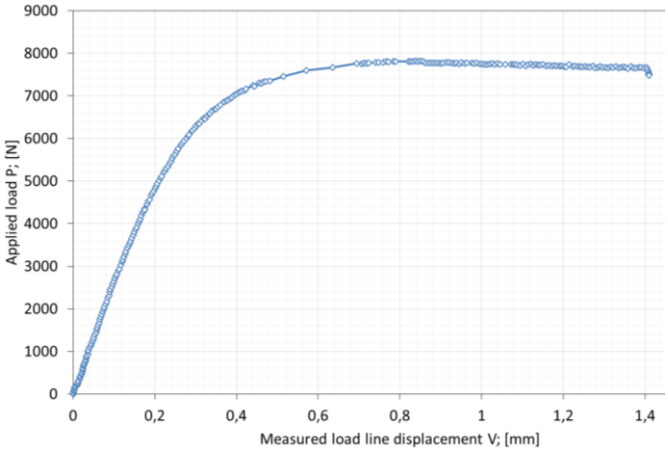

Figure 7. Diagram F-V after PWHT

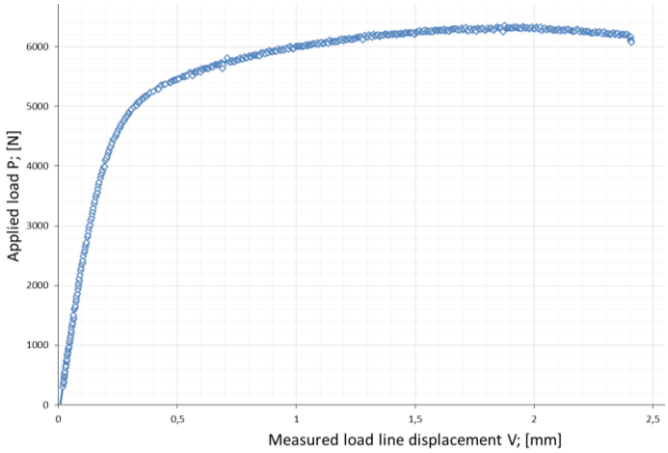

Figure 8. Diagram F-V after PWHT

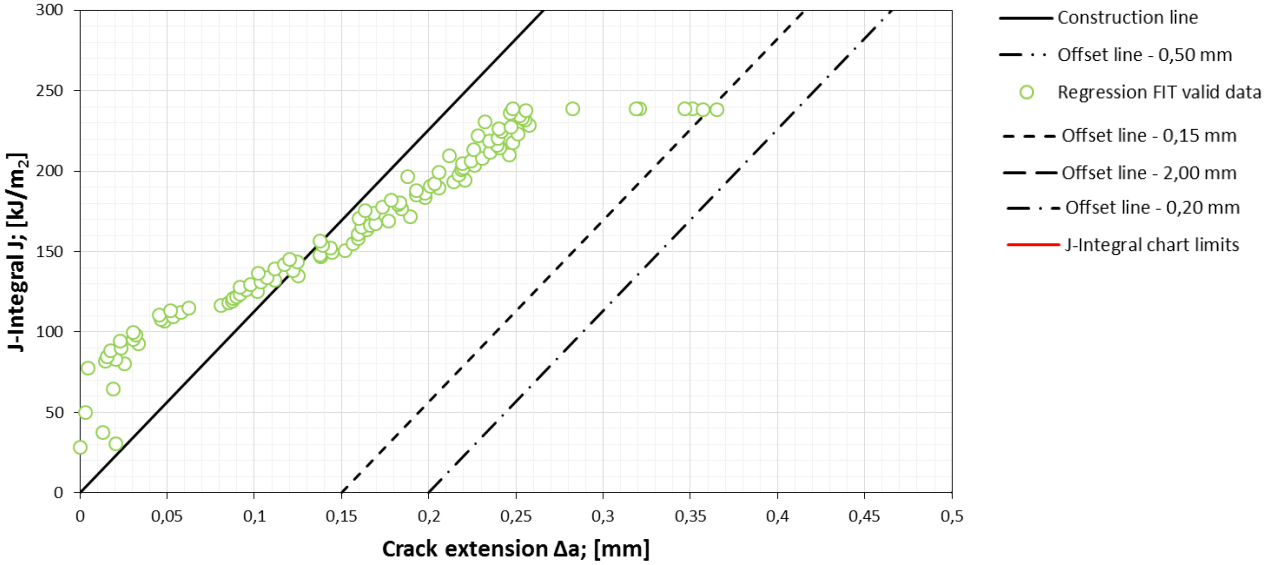

Figure 9. The J-R curve before PWHT.

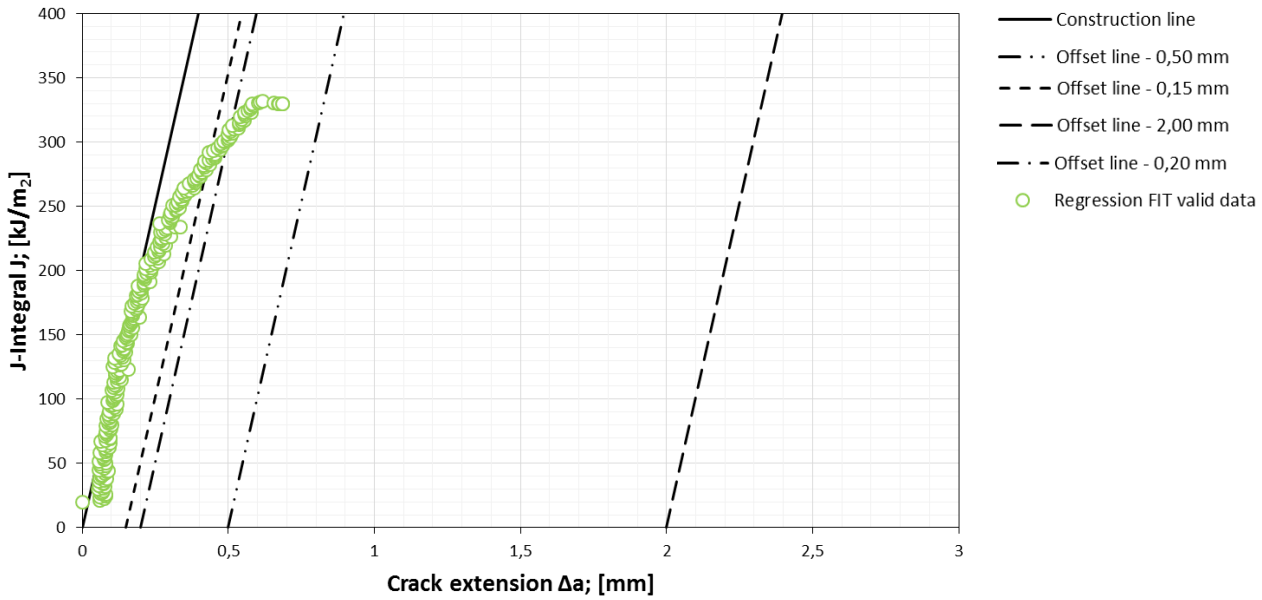

Figure 10. The J-R curve after PWHT.

Results were processed in accordance with the ASTM E1820 standard. Figures 9 and 10 show typical curves for determining fracture toughness according to the fracture behaviour for the test CT specimen. Critical values of fracture toughness for each test specimen are shown in Table 5. Obtained values of fracture toughness K_{Ic} can be used as critical values for assessing the structural integrity of the vessel head. Numerically and analytically calculated SIF presented in Table 5 show a good matching.

Numerical analysis and calculation of SIF

The numerical calculation of the stress intensity factor (SIF) for the crack location on the cylindrical part and on the spherical part of the vessel head is carried out using Ansys® software. For adopted vessel dimensions with diame

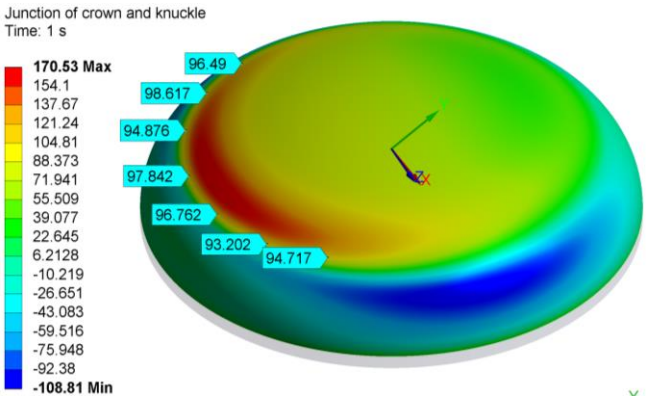

Figure 11. Circumferential stress distribution

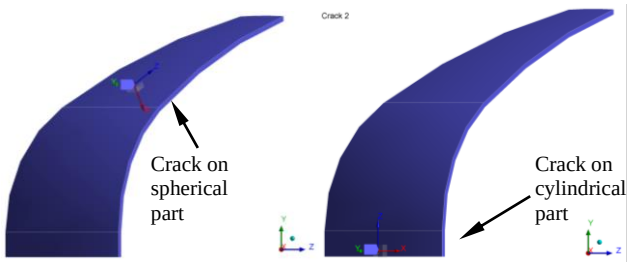

Figure 12. Crack position on vessel head.

ter D = 1875 mm, wall thickness t = 10 mm, material P355, and effective internal pressure p = 12.6 bar, the results are illustrated in Figs. 11, 12 and 13. The starting crack is semi-elliptical with sizes a = 5 mm and 2c = 10 mm placed in the meridional direction. Crack opening is in the circular direction.

Table 5. Results of SIF factor for primary stress.

Spherical part		Cylindrical part	
SIF according to FEM			
$K_{1sphere}$ (MPa√mm)	$K_{1sphere}$ (MPa√m)	$K_{1cylinder}$ (MPa√mm)	$K_{1cylinder}$ (MPa√m)
264	8.4	338	10.7
SIF from Eq.(6) calculated for primary stress σ_φ			
225	7.25	299	9.5

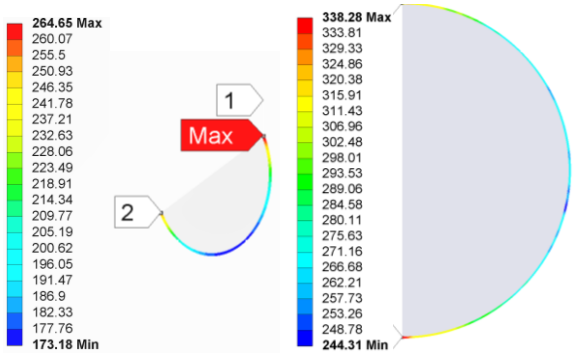

Figure 13. Stress intensity factor (SIF).

Fracture safety assessment

Structural integrity assessment of the pressure vessel head is performed using the failure assessment diagram, /7/. Considering that the analysis is carried out using a conservative approach, the cracks that are the subject of analysis are linear-isolated semi-elliptical surface cracks. This analysis considers the existence of welding residual stresses when determining the K_r parameter. The failure assessment diagram defines the boundary between two independent solutions, which predict fully brittle fracture based on LEFM (parameter K_r), and failure of the structure due to plastic

collapse defined by plasticity analysis (parameter S_r). The calculation of the brittle fracture parameter, K_r, is defined according to:

$$K_r = \frac{K_I}{K_{Ic}}. \quad (4)$$

Based on the calculated values, the variables: S_r and K_r are defined, and the equation is obtained:

$$K_r = S_r \left[\frac{8}{\pi^2} \ln \sec\left(\frac{\pi}{2} S_r \right) \right]^{\frac{1}{2}}. \quad (5)$$

The stress intensity factor K_I (by taking approximately into account geometry and load) is determined for the data given in Table 6 by the equation:

$$K_I = \sigma \sqrt{\frac{\pi a}{Q}}, \quad (6)$$

where: $\sigma_{tot} = (\sigma_\varphi + \sigma_{res\text{-}\varphi})$ (MPa), primary and residual stress; $\sigma_\varphi = \frac{p_i R_t}{t}\left[1 - \frac{R_t}{2R_L}\right]$ (MPa), primary tangential stress on spherical part of vessel head, /10/, Table 6; $\sigma_\varphi = p_i R/t$ (MPa), primary tangential stress on cylindrical part of vessel head, /10/, Table 6; $\sigma_{res\text{-}\varphi}$ (MPa), component of residual stress defined from the equation of Mohr's circle, perpendicular to the weld; $Q = 1 + 1.464(a/c)^{1.65}$, approximate geometrical factor for $a \le c$; other correction factors are ignored; $a = t/2$ (mm), appropriated crack depth that corresponds to half the thickness of the vessel head; $a/2c = 0.5$, crack dimensions; $p_i = 1.26$ MPa, operating internal pressure; $R_t = \left[\frac{R^4}{h^2} + \left(1 - \frac{R^2}{h^2}\right) x^2 \right]^{0.5}$, radius of curvature; $R_L = \frac{R_t^3 h^2}{R^4}$, radius of curvature; $x = 400$ mm, crack distance from the head axis; $r = 0.154D$, radius of the torus; $L = 0.8D$ (mm), radius of spherical part of head; $R = D/2$ (mm), radius of vessel head; $D = 1875$ mm, diameter of vessel head; $t = 10$ mm, wall thickness; K_{Ic} (MPa√m), fracture toughness determined indirectly using J_{Ic}, defined and presented in Table 6.

The problem is observed for cracks located in the axial direction of the welded joint, i.e., the meridional direction on vessel head. Considering the dimensions of the vessel head, the influence of contour curvature (section) can be ignored. With these approximations, the problem is reduced to a tensioned plate whose dimensions are significantly larger than the length of the crack.

Active stresses (operating and residual stresses) that open the crack have a circular direction. Other data required for a complete assessment of structural integrity using the failure assessment diagram are presented in Table 6.

Calculation of plastic collapse parameter, S_r, is performed according to the equation:

$$S_r = \frac{\sigma_n}{\sigma_F}, \quad (7)$$

where: $\sigma_n = (1 + a/t)\sigma_\varphi = 1.5\sigma_\varphi$ (MPa), is the primary stress created because of the action of internal pressure increased by stress concentration; $\sigma_F = (R_{eH} + R_m)/2$ (MPa), is plastic collapse stress expressed as the mean sum of yield stress and tensile strength obtained by tension test.

Table 6. Calculated values of parameters K_r and S_r before/after PWHT.

Crack size	Inner pressure	Primary stress	Secondary stress	Total stress	Stress intensity factor for σ_{tot}	Fracture toughness	Parameter	Primary stress with stress concentration	Plastic failure stress	Parameter
$a/2c$ (-)	p_i (MPa)	σ_φ (MPa)	$\sigma_{res\text{-}\varphi}$ (MPa)	σ_{tot} (MPa)	K_I (MPa√m)	K_{JIc} (MPa√m)	K_r	σ_n (MPa)	σ_F (MPa)	S_r
Before PHWT-spherical part of vessel head										
0.5	1.26	89	333	422	33.7	41.1	0.82	101	579	0.23
Before PHWT -cylindrical part of vessel head										
0.5	1.26	120	333	452	36.1	41.1	0.88	180	579	0.3
After PHWT -spherical part of vessel head										
0.5	1.26	89	161	250	19.9	42.9	0.49	101	512	0.26
After PHWT - cylindrical part of vessel head										
0.5	1.26	120	161	281	22.4	42.9	0.55	180	512	0.4

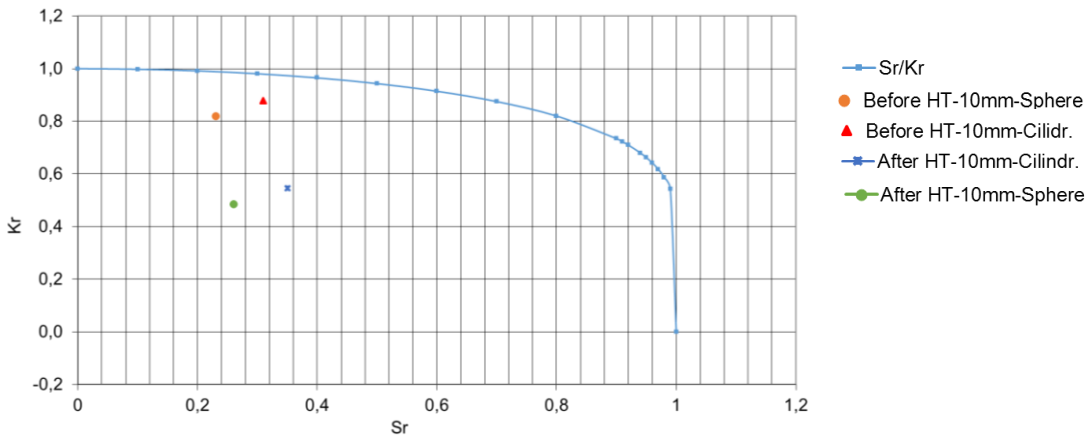

Figure 14. Failure assessment diagram.

Considering that it is a very conservative approach it aims to prove in the simplest and safest way whether the integrity of the structure is safe or not. Values of parameters K_r and S_r calculated for cracks corresponding to half the thickness of the vessel head for samples taken before PWHT are in the safe area, within the limit curve. Results for samples taken after PWHT are worse and beyond the acceptable limit for given sheet thickness, Fig. 14.

DISCUSSION

Based on performed test results presented in Tables 4-6 and Fig. 14, the following can be noted:

- very good agreement between numerical and analytical results of SIF;
- uniform hardness was measured before and after PWHT;
- values of mechanical properties of samples are above minimal standard values of R_{eH} = 408-421 MPa for steel P355NL2+H (according to material certificate). Plastic deformation led to material strengthening and increase in yield stress and tensile strength. Heat treatment reduced mechanical properties. Test samples broke in the HAZ;
- incremental deformation and welding introduced significant residual tensile stresses. Lower residual stress values were measured on samples after PWHT;
- uniform impact energy properties before and after PWHT corresponding to tough material;
- the results show that K_{JIc} values are relatively low which is most likely a consequence of fatigue crack tip location in HAZ. Measured fracture toughness Values K_{JIc} do not change significantly due to the effect of PWHT;
- low resistance to the existence of a crack.

CONCLUSIONS

Observing all the results of the tests performed before and after the post weld heat treatment (PWHT), it can be concluded that the thermal treatment did not significantly improve the mechanical properties. The most significant effect was reducing the magnitude of residual stress. Also, the structural integrity assessment results given in the FAD diagram for samples after PWHT are better compared to the results obtained before PWHT. Production process and welding introduced dominant tensile residual stress, that negatively affect the increase in the risk of cracks.

Considering the conservatism in the assessment of the structural integrity, the vessel heads before PWHT are near to limit of acceptability and being more tendency to brittle fracture than plastic collapse. The reduction of residual stresses after PWHT had a suitable effect on the structural integrity, and in this case the vessel heads are safe from brittle fracture and plastic collapse.

ACKNOWLEDGEMENT

The research was supported by Metacomm Jajce d.o.o., Bage 5, 70101 Jajce, Bosnia and Herzegovina, email: metacomm.jajce@gmail.com ; www.metacomm-bih.com.

REFERENCES

1. Matsubara, S. (1994), *Incremental backward bulge forming of a sheet metal with a hemispherical head tool*, J Japan Soc. Technol. Plasticity, 35(406): 1311-1316.
2. Iseki, H., Kumon, H. (1994), *Forming limit of incremental sheet metal stretch forming using spherical rollers*, J Japan Soc. Technol. Plasticity, 35(406): 1336-1341.
3. Rojek, J., Kleiber, M., Piela, A., et al. (2004), *Deterministic and stochastic analysis of failure in sheet metal forming operations*, Steel Grips 2, Suppl. Met. Forming: 29-34.
4. Alhassan, M., Bashiru, Y. (2021), *Carbon equivalent fundamentals in evaluating the weldability of microalloy and low alloy steels*, World J Eng. Technol. 9(4): 782-792. doi: 10.4236/wjet.2021.94054.
5. Hance, B.M., *The influence of deformation-induced residual stresses on the post-forming tensile stress/strain behavior of dual-phase steels*, Doctoral Dissertation, University of Pittsburgh, School of Engineering, 2005.
6. Ištvanić, Z., *Contribution to the assessment of integrity of cylindrical dish ends made by the incremental sheet metal forming* (in Bosnian), Doctoral Dissertation. University of Zenica, Bosnia and Herzegovina, 2022.
7. Anderson, T.L., Fracture Mechanics - Fundaments and Applications, 3rd Ed., CRC Press, Taylor and Francis Group, 2005.
8. Vukojević, D., Vukojević, N., Lemeš, S., Ištvanić, Z. (2007), *Analysis of tool radius on vessel head quality made by incremental plastic deformation*, In: Proc. 11th Int. Research/Expert Conf. 'Trends in the Development of Machinery and Associated Technology', TMT 2007, Hammamet, Tunisia, 2007, pp.87-90.
9. Vukojević, D., Vukojević, N., Hadžikadunić, F., Ištvanić, Z. (2007), *Some aspects of spherical vessel head quality made by incremental deformation treatment*, In: Proc. 5th Research/ Expert Conf. Quality 2007, pp.299-304.
10. Bednar, H.H., Pressure Vessel Design Handbook, Van Nostrand Reinhold Comp, New York, 1986.
11. EN ISO 4063:2009. Welding and allied processes - Nomenclature of processes and reference numbers (ISO 4063:2009, Corrected version 2010-03-01; EN ISO 4063:2010)
12. DIN 28013:1993. Ellipsoidal Dished Ends, Beuth Verlag GmbH, Berlin.
13. BAS EN ISO 6507-1:2018. Metallic materials - Vickers hardness test - Part 1: Test method.
14. BAS EN ISO 6892-1:2017 B: Metallic materials - Tensile testing - Part 1: Method of test at room temperature.
15. BAS EN ISO 4136:2014: Destructive tests on welds in metallic materials - Transverse tensile test.
16. ISO 148-1:2016: Metallic materials - Charpy pendulum impact test - Part 1: Test method
17. BAS EN ISO 9016:2012: Destructive tests on welds in metallic materials - Impact tests - Test specimen location, notch orientation and examination.
18. ASTM 837:2013. Standard test method for determining residual stresses by the hole-drilling strain-gage method.
19. ASTM E1820:2018. Standard test method for measurement of fracture toughness. Plane stress/Plane strain.
20. ASTM E 399:2022. Standard test method for linear –elastic plane-strain fracture toughness of metallic materials.
21. EN 14171:2002. Welding consumables. Wire electrodes and wire-flux combinations for submerged arc welding of non-alloy and fine grain steels.